26th ABCM International Congress of Mechanical Engineering
November 22-26, 2021. Florianópolis, SC, Brazil

COB-2021-0890
A METHODOLOGY TO FIELD TESTING FRICTION BETWEEN ALUMINUM WIRES AND WHEELS OF CABLE RIDING ROBOTS

Marina Baldissera de Souza
Gustavo Queiroz Fernandes
Rodrigo de Souza Vieira
Lauro Cesar Nicolazzi
Universidade Federal de Santa Catarina, Departamento de Engenharia Mecânica, Centro Tecnológico, Campus Universitário - Trindade, CEP: 88.040-900, Florianópolis/SC - Brasil
marina.bs@posgrad.ufsc.br - gustavo.fernandes@posgrad.ufsc.br - rodrigo.vieira@ufsc.br - lauro.nicolazzi@ufsc.br

Roberto Kinceler
Alessandro Pedro Dadam
Celesc Distribuição S.A., Florianópolis/SC - Brasil
rkinceler@celesc.com.br - alessandropd@celesc.com.br

Abstract. *The failure of any electrical component of overhead power lines may lead to the inefficiency or even to the complete interruption of energy distribution. Robotic systems for inspecting overhead power lines have been designed in an attempt to automate the inspection process and make it faster and more reliable. Most of the robotic systems rely on wheels to move along the conductors of overhead lines. Thus, the friction coefficient of the contact wheel-wire plays a fundamental role for the proper design of those robots. Preventing slippage in both dry and wet conditions, precisely selecting traction motors and developing the control system are some of the design steps that depend on knowing the friction coefficient. This paper proposes a method to estimate the static friction and the rolling resistance coefficients between the surfaces of a robot's wheel and a conductor wire cable. The measurement is made in a field test, where a mass is attached to a wheel's replica through a rope parallel to the conductor. A real standard conductor cable connects two poles with different heights. The mass is carefully increased until it slightly pulls the replica along the conductor. The mass' weight that moves the replica determines the friction coefficients. A Polyurethane wheel of 50 Shore A hardness is used as case study, considering dry and wet conditions. Average values for static and rolling friction coefficients for both conditions are obtained. The impact of the water on the static friction is quantified, aiding to define the robot's operation conditions. The method proved to be effective for estimating a friction coefficient, as it has simple execution and it does not require special equipment, so it can be easily performed in any environment involving wheels and wire ropes.*

Keywords: *inspection robot, friction on wire cables, friction coefficient, inclined plane, overhead power lines*

1. INTRODUCTION

The failure of any electrical component of overhead power lines may lead to the inefficiency or even to the complete interruption of energy distribution, representing financial risks for both electrical utility companies and citizens (Alhassan *et al.*, 2020). Consequently, a vast amount of bibliography on different inspection robotic systems for overhead power lines has been produced since the 1990's in an attempt to automate the inspection process and make it faster and more reliable. Some of the most recent works that can be found in the literature related to the development of robots to inspect power lines are presented by Zhang *et al.* (2020), Wang *et al.* (2019), Gulzar *et al.* (2018), Mirallès *et al.* (2018), Chang *et al.* (2017), Qing *et al.* (2016), Mostashfi *et al.* (2014) and Boje (2014).

A few of the aforementioned works may deal with the development of drones in order to improve mobility of the robotic system and avoid the difficulties of obstacle crossing. However, these solutions usually run into the problem of autonomy, as drones have limited time of flying between charges, and of space, since there may be buildings and trees surrounding the overhead lines hindering the operation, especially into distribution lines (Alhassan *et al.*, 2020). In addition, drones must also respect local regulations which impose rules such as not flying over people, maximum payload, altitude and speed, minimum lateral distance from any obstacle, operation only in daylight hours and by licensed pilots (Shakhatreh *et al.*, 2019). Consequently, the robotic systems that try to keep the advantages of drones usually end up with hybrid solutions, such as the robots proposed by Wang *et al.* (2019) and Chang *et al.* (2017), both with the capability of flying during transposition of poles and the necessary degrees of freedom and tools to move along the conductors of the

power lines.

Due to these constraints of operating drones, most of the robotic systems found in the literature rely on the use of wheels to allow its movement along the conductors of the overhead lines. Thus, the friction coefficient resulting from the contact wheel-wire plays a fundamental role for the proper design of those robots. It is the static friction coefficient that allows the prevention of slippage (Morozovsky and Bewley, 2013). The first prototype of the Expliner robot, for example, presented slippage as the rubber coating of the wheels did not provide enough friction with the wires (Debenest *et al.*, 2008). Similarly, the first versions of the cable-crawler robot created by Bühringer *et al.* (2010) could not traverse the mast tip due to obstacle geometry and insufficient friction. In both cases, the problems were solved with changes in the designs so that the obtained friction between wheels and wire were higher than a minimum value required for each application. Moreover, this minimum friction coefficient for traction has also to be assessed for wet conditions as rain, snow and other climatic elements may impact the friction coefficient and create more difficulties for the motion of the robot (Montambault and Pouliot, 2010).

Beyond guaranteeing a minimum friction to avoid slippage for both dry and wet conditions, an accurate estimation of the friction coefficient contributes for a more precise sizing and selection of traction motors and aids the development of the control system (Gulzar *et al.*, 2018; Gao *et al.*, 2020; Alhassan *et al.*, 2020; Xiao *et al.*, 2016). Therefore, measuring the friction between wheels and wire cable is essential in the project of inspection robots for overhead power lines. However, in spite of being crucial in inspection robots design, the authors have not found any work on measuring friction and/or tractive effort between robot's wheels and aluminum wire cables. Many works focus on robot kinematics and trajectory development to avoid obstacles, without considering the efforts in the interaction between wheel and cable (Tsujimura *et al.*, 1996; Nayyerloo *et al.*, 2007; Pouliot and Montambault, 2008; Li *et al.*, 2009; Yang *et al.*, 2012; Goncalves and Carvalho, 2015). Song *et al.* (2012) stand out by including force constraints in the solution of the inverse kinematics of the transmission line maintenance robot AApe-D. One force constraint is related to the friction between wheels and cable. Although taking into account friction effect in calculation, some experiments of the AApe-D running along the line and crossing obstacles were carried out but the authors do not explain if or how the friction is evaluated.

Other analyses found in literature which consider the friction between wheels and cables in robot projects do not delve deeper into the issue. Yifeng *et al.* (2011) conduct a simulation to evaluate the influence of the driving wheel on increasing climbing capability, which is related to the wheel material. However, they do not try different materials and, consequently, they do not change the friction coefficient. Morozovsky and Bewley (2013) analyze the dynamics and build a prototype of the SkySweeper, a mobile robot designed to operate in an environment of ropes, cables and wires. They added a thin layer of silicone rubber to the ABS plastic roller in contact with the wire cable to increase friction without conducting any tests to verify if the silicone was the best choice.

Perhaps the main reason behind the lack of experiments to evaluate the friction between robot's wheels and conductor is the difficulty to reproduce the wire cable surface in laboratory. Using traditional equipment to measure friction coefficient, such as a tribometer, would demand modifying the samples' geometry and positioning. The modification could lead to an arrangement too distant from the real environment of overhead power lines. As a result, experiments to measure wear and friction of wire cables demand a self-made test rig, even in applications outside distribution and transmission lines. One example is mine hoisting systems, where steel wires are widely used and are subjected to diverse conditions. Each research on friction and wear behaviors of steel wires needed specific test rigs depending on the experiment goal, e.g. measuring friction coefficient (Xu *et al.*, 2019; Chang *et al.*, 2016; Stawowiak and Żołnierz, 2018) or evaluating the corrosion (Chang *et al.*, 2020) and the impact load effects (Peng *et al.*, 2018).

With all this in mind, this paper proposes a simple method to estimate the static friction coefficient and the rolling resistance coefficient between the surfaces of a robot's wheel and a conductor wire cable. The method is based on the inclined plane principle, already used to measure friction coefficient. The measurement is made in a field test, by weighting the minimal mass necessary to slightly pull a wheel's replica along a real standard conductor cable. The cable connects two poles with different heights.

The remainder of this paper is structured as follows. Some methods currently used to measure friction coefficient are described in Section 2. Section 3. presents the mathematical development of the equations needed to estimate the friction coefficient between the robot's wheel and the conductor cable. Moreover, the procedure to conduct the test field is detailed in this section. A study case is presented in Section 4. in which the rolling resistance and static friction coefficients between the surfaces of a Polyurethane wheel and of an aluminum wire cable are measured in dry and wet conditions. Finally, some conclusions are drawn in Section 5.

2. CURRENT METHODS FOR MEASURING FRICTION COEFFICIENT

The physical principles behind measuring friction coefficients are given by the phenomenon being evaluated: static friction, dynamic friction or rolling resistance. The standard ASTM G11510 assembles multiple tests to measure friction coefficient. The standard includes the procedure of placing a rider on an inclined structure whose angle of inclination increases until the rider moves. At this moment, the tangent of the angle gives the static friction coefficient. The rider's movement is observed with the unaided eye (Budinski, 2005). Some Brazilian standards also propose methods based on

an inclined plane to measure static friction coefficient (ABNT NBR 13989; ABNT NBR ISO 12957-2).

Standard ABNT NBR 11992 presents a method to determine the static friction coefficient between hoses for unblocking and cleaning and the internal surface of PVC pipes for sanitary sewage. The method principle consists of attaching a container to an extremity of a rope and a hose specimen to the other. The rope passes through a pulley. The container load is carefully increased until the static equilibrium is broken. The ratio between the container weight and the specimen weight defines the static friction coefficient.

Standard ABNT NBR 16643 describes a test bench to measure dynamic friction coefficient of microducts. A section of a microduct is supported on an arc section of a pulley. A fixed weight is attached to one extremity of the microduct and a variable force is applied on the other extremity until the microduct starts moving. The dynamic friction coefficient is estimated from the data collected at this moment.

In the scientific literature, Alió-Sanz *et al.* (2016) used the inclined plane principle to evaluate friction between a bracket and an arc wire. The friction is assessed according to the time and distance traveled by the brackets on an inclined stainless steel wire.

Based on standards ABNT NBR 16643:2017 and ABNT NBR 11992:2017 and on the experiments of Alió-Sanz *et al.* (2016), we developed the methodology described in Section 3.to measure the static friction coefficient and the rolling resistance coefficient between the surfaces of robots' wheels and aluminum wire-cables.

3. METHODOLOGY

A schematic representation of the field test arrangement is shown in Fig. 1. The friction is field tested on a de-energized duplicate of a distribution power line with poles at different heights. An aluminum wire rope, coming from a distribution power line, connects the two poles. A replica of the robot's wheel is placed on the conductor. The replica is mounted on a structure with a hook to attach a set of masses in order to simulate the robot total weight. A support is placed behind the replica to prevent the wheel from rolling in direction to the lower pole. A pulley is attached to the crosshead of the higher pole and a rope is wrapped around the pulley. One end of the rope is tied to the structure where the replica is mounted on and the other end is tied to a container where water will be poured.

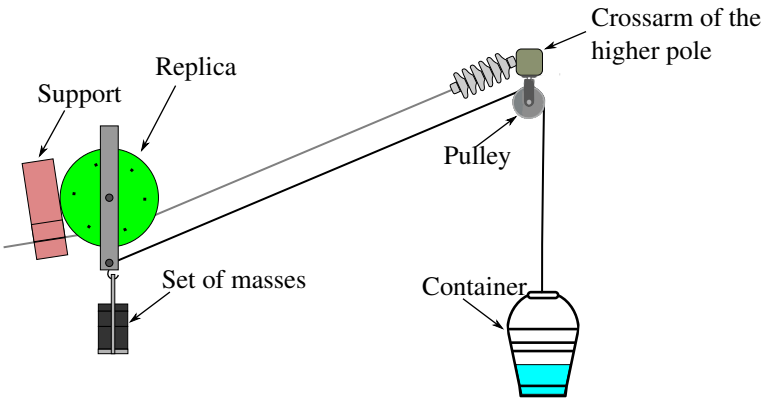

Figure 1. Schematic representation of the field test arrangement

The principle behind the method is pouring water in the container until the static equilibrium of the replica is broken. The friction force and the friction coefficient are then computed from the replica and water weights and from the wire's inclination angle in relation to the ground. Before carrying out this experiment, the rolling resistance coefficient of the pulley bearing must be estimated and taken into consideration in order to avoid oversized measurements of the wheel-wire friction coefficient. Consequently, the specification of the robot's required traction motor is not oversized.

3.1 Rolling resistance of the pulley bearing

The rolling resistance coefficient of the pulley bearing is quantified through a test whose schematic representation is shown in Fig. 2. A rope wraps the pulley and a small receptacle is attached to each end of the rope. The two receptacles are identical. The first step of the test consists of pouring the same amount of water in the two receptacles, so that the both are in static equilibrium, i.e. both have the same weight ($W_1 = W_2$), as illustrated in Fig. 2(a). This step also guarantees that the rope connecting both receptacles is tractioned. The second step consists of pouring water slowly and carefully in one of the receptacles until the static equilibrium is broken. The heavier receptacle, with weight W_1, goes down and makes the lighter receptacle, with weight W_2, to go up. The second step is represented in Fig. 2(b).

The rolling resistance coefficient f_b of the pulley bearing is determined from the weight difference ΔW which provoked the vertical displacement. f_b is obtained through Newton's 2^{nd} Law. Fig. 3 shows the free body diagram of the bearing.

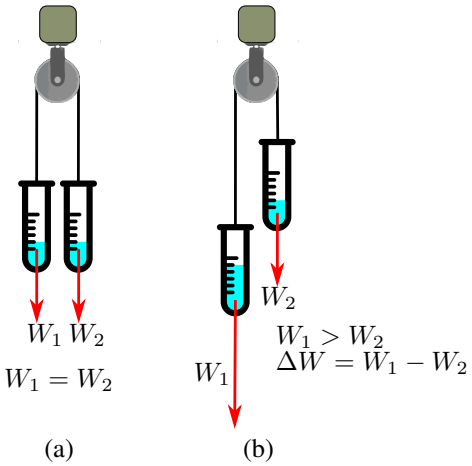

Figure 2. Schematic representation of the test to measure the rolling resistance coefficient of the pulley bearing. In (a), both receptacles weigh the same. In (b), the receptacle at the left is heavier than the receptacle at the right, provoking the vertical displacement in both receptacles

In Fig. 3(a), the forces acting on the bearing are the weight difference ΔW; the normal force N_b, which is the reaction to the receptacles weights, so $N_b = W_1 + W_2$; and the rolling resistance force F_{f_b} between the shaft and the bearing, resisting the pulley's rotation. The forces ΔW and F_{f_b} create the moments $M_{\Delta W}$ and M_{f_b}, respectively, at the bearing center. The moments are shown in Fig. 3(b). The moment equilibrium gives:

$$M_{f_b} = M_{\Delta W} \tag{1}$$

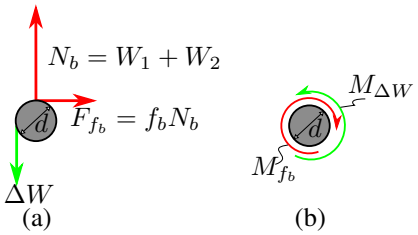

Figure 3. Free body diagram of the pulley bearing, representing (a) the forces and (b) the moments that act on it

Knowing that the bearing diameter is d:

$$\begin{cases} M_{f_b} = F_{f_b} \frac{d}{2} \\ M_{\Delta W} = \Delta W \frac{d}{2} \end{cases} \tag{2}$$

The rolling resistance force is the product $F_{f_b} = f_b N_b$. Knowing that $N_b = W_1 + W_2$, by replacing these equalities and Eq. 2 in Eq. 1, we have $f_b(W_1 + W_2)\frac{d}{2} = \Delta W$, resulting in:

$$f_b = \frac{\Delta W}{W_1 + W_2} = \frac{W_1 - W_2}{W_1 + W_2} \tag{3}$$

Therefore, the rolling resistance coefficient of the bearing is given by the ratio between the difference of weight of the receptacles and the sum of both weights.

3.2 Friction between wheels and wire cable

After estimating the rolling resistance coefficient of the pulley bearing, the friction between the surfaces of the replica and of the wire cable is evaluated. Fig. 4 presents the forces involved in the test. There are four forces acting on the replica: its own weight W_{wheel}, the normal force N_{wheel} generated by the support of the replica on the wire rope, the friction force F_f and a traction force T_1. There are two forces acting on the container: the container's own weight W_{water} and another traction force T_2. It is supposed that the rope is inextensible and the single reason behind the changing of the force transmitted by the rope is the friction of the pulley's bearing. The angle α is the conductor inclination in respect to a horizontal line parallel to the ground. The inclination comes from the height difference of the poles and from the sag of the cable due to the wheel's weight.

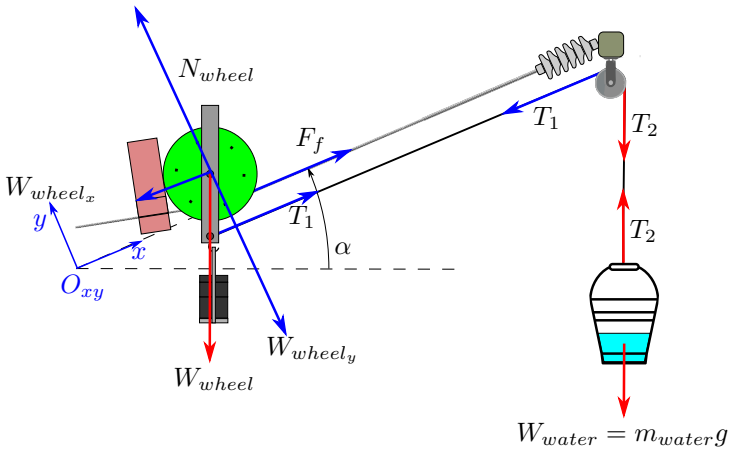

Figure 4. Forces involved in the field test

The replica weight is defined as $W_{wheel} = m_{wheel}g$, where m_{wheel} is the replica's mass and g the gravity acceleration. The weight W_{wheel} can be decomposed according to the frame O_{xy} shown in Fig. 4. The component parallel to the y-axis and normal to the conductor is calculated as $W_{wheel_y} = W_{wheel}\cos\alpha$. The component parallel to the x-axis and tangential to the conductor is $W_{wheel_x} = W_{wheel}\sin\alpha$. The replica is in static equilibrium. So, the component W_{wheel_y} is equal to the normal force N_{wheel} acting on the replica. The normal force N_{wheel} determines the friction force F_f, as F_f is the product between an adimensional coefficient ϱ and the normal force:

$$F_f = \varrho N_{wheel} \tag{4}$$

In this paper, ϱ can be the static friction coefficient or the rolling resistance coefficient. The development of the equations is the same for both coefficients, so we use ϱ to refer to anyone of them.

Since the replica is on static equilibrium, the friction force F_f is calculated as:

$$F_f = W_{wheel_x} - T_1 \tag{5}$$

The container is also in static equilibrium. So, the traction force T_2 is equal to the container's weight:

$$T_2 = W_{water} = m_{water}g \tag{6}$$

where m_{water} is the mass of the container with water.

The Newton's 2^{nd} Law is applied to the pulley's bearing to compute the friction force F_f and friction coefficient ϱ. Fig. 5(a) contains the free body diagram of the bearing, considering the forces represented in Fig. 4.

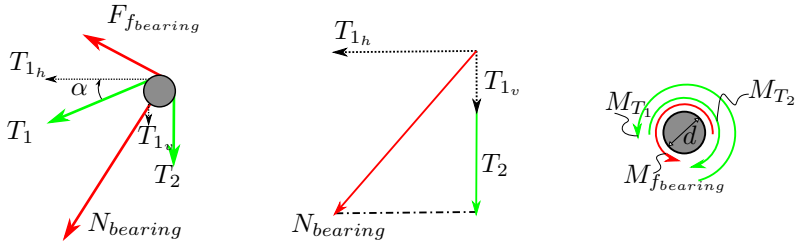

(a) (b) (c)

Figure 5. Free body diagram of the pulley bearing, representing (a) the forces acting on it during the field test, (b) the composition of the force normal to the bearing, $N_{bearing}$ and (c) the moments that act on it during the test field

During the field test, the pulley's bearing is submitted to the traction forces T_1 and T_2, to a force normal to the bearing surface, $N_{bearing}$, and to the rolling resistance between the pulley's shaft and the bearing, $F_{f_{bearing}}$. T_1 is parallel to the conductor and can be decomposed into $T_{1_h} = T_1\cos\alpha$, parallel to the ground, and $T_{1_v} = T_1\sin\alpha$, perpendicular to the ground. The force $F_{f_{bearing}}$ is calculated through the product $F_{f_{bearing}} = f_b N_{bearing}$. Fig. 5(b) shows the forces composing $N_{bearing}$, whose magnitude is given by:

$$N_{bearing} = \sqrt{T_{1_h}^2 + (T_{1_v} + T_2)^2} \tag{7}$$

Figure 5(c) contains the free body diagram of the bearing with the moments that act on its center during the test field. The moment $M_{f_{bearing}}$ is generated by the friction force $F_{f_{bearing}}$ and the moments M_{T_1} and M_{T_2} are generated by T_1 and T_2, respectively. These three moments are computed as:

$$\begin{array}{l} M_{f_{bearing}} = F_{f_{bearing}} \frac{d}{2} = f_b N_{bearing} \frac{d}{2} \\ M_{T_1} = T_1 \frac{d}{2} \\ M_{T_2} = T_2 \frac{d}{2} \end{array} \tag{8}$$

Applying Newton's 2^{nd} Law:

$$M_{f_{bearing}} + M_{T_1} - M_{T_2} = 0 \tag{9}$$

Replacing Eq. (7) in Eq. (8) and then substituting Eq.(8) in Eq.(9), we have:

$$f_b \sqrt{T_{1_h}^2 + (T_{1_v} + T_2)^2} = T_2 - T_1 \tag{10}$$

After some algebraic manipulation, a quadratic equation emerges:

$$(f_b^2 - 1)T_1^2 + 2T_2(f_b^2 \sin\alpha + 1)T_1 + (f_b^2 - 1)T_2^2 = 0 \tag{11}$$

Since f_b, α and T_2 are known, the quadratic equation's unknown is T_1 in Eq. (11). Eq. (11) has two solutions and the value that gives the lowest friction force F_f should be chosen. The reason behind this criterion is that the quadratic equation considers the friction moment $M_{f_{bearing}}$ acting in both senses, with one root for each sense (clockwise and counterclockwise). The higher root considers $M_{f_{bearing}}$ has the same sense of the motion and M_{T_2}. For this situation, T_1 has to assume a higher value in order to lead to a moment that compensates both M_{T_2} and $M_{f_{bearing}}$. However, the friction always opposes the movement, condition represented by the lower root. In this case, T_1 is smaller because it has to create a moment that is equivalent to the difference of $M_{f_{bearing}}$ and M_{T_2} and f_b, as indicated in Fig. 5(c).

Finally, the chosen value of T_1 is replaced in Eq. (5) to determine the friction force F_f between the replica and the conductor. The friction coefficient ϱ is defined using the resulting F_f: $\varrho = F_f / N_{wheel}$.

3.3 Procedure to evaluate friction between wheel and wire cable

An experimental apparatus based on the schematic view of Fig. 1 was built on a power network used for tests at UFSC. The tests consisted of pourishing water in the container until the replica starts to move away from the support. As soon as the motion starts, the deposition of water in the container stops and the water container is weighed with a precision scale. The friction coefficient was determined according to the mathematical formulation described in Section 3.2 The test results indicate the maximum friction force that must be exceeded for the replica to start moving.

The test procedure is divided into four main steps: the first step consists of preparing the apparatus in the power network, the next two steps comprise carrying out the experiments and the last step is for the statistical analysis and estimation of the friction coefficients. The two intermediate steps were planned so that two frictional forces could be estimated, as follows:

- Static friction force: friction force that arises when the wheel slides over the conductor. For these tests, the rotation of the wheel along its rotation axis is prevented so that the static friction phenomenon can be evaluated;
- Rolling resistance force: friction force that arises when the wheel rolls over the conductor. For these tests, the rotation of the wheel along its rotation axis is not prevented, such that the rolling resistance phenomenon can be evaluated.

The complete procedure for each of the four steps is presented below:

STEP 1 - Preparation Procedures

1. Measure the original wire inclination at the point where the replica will be positioned and the frictional forces measured;
2. Install the support in this point, so that it will prevent the wheel from rolling back;
3. Install the pulley to the superior crosshead;
4. Attach the weights to the replica. These weights allow the wheel to simulate the contact condition that will be observed for the real cable climbing robot;

5. Place the replica (wheel and weights) on the line, leaning against the support;
6. Tie one end of the rope to the replica;
7. Pass the rope through the pulley, so that:
   (a) The portion of the rope between the replica and the pulley is parallel to the conductor. Perform leveling of the pulley as needed;
   (b) The rest of the rope, from the pulley to the rope's free end, is vertical/parallel to the pole.
8. Tie the container to the free end of the rope;
9. Pour water into the container until the rope is tractioned;
10. Adjust the angle of the rope already tractioned so that it is parallel to the conductor. Leveling of the pulley fixed to the crosshead may again be performed;
11. Measure the wire angle near the replica with the aid of a level;
12. Check if the system is in static balance.

STEP 2 - Procedures for Measuring the Rolling Resistance

1. Pour water into the container cautiously until the replica starts to roll. Stop pouring water as soon as the model moves away from the support;
2. Measure the mass of the water container;
3. Record balance result;
4. Perform 10 repetitions of the steps 2.1 to 2.3.

STEP 3 - Procedures for Measuring the Static Friction Force

1. Lock the replica's rotation axis;
2. Pour water cautiously into the container until the wheel starts to slide. Stop pouring water as soon as the model moves away from the support;
3. Measure the mass of the water container;
4. Record balance result;
5. Perform 10 repetitions of the steps 3.1 to 3.4.

STEP 4 - Statistical Analysis

- With the values obtained in the previous two procedures, the friction forces and the friction coefficients are calculated. The maximum and the minimum values, the arithmetic mean, the mode and the standard deviation are also computed from the results. A scatter plot is generated for better understanding of the results, with the wire inclination angle on the abscissa axis and the friction coefficient on the ordinate axis.

As it can be seen in the procedure, steps 2 and 3 suggest 10 repetitions each for the measurement of friction forces. This is intended to minimize the impact of noisy measurements in the estimated friction forces and, consequently, to reduce the uncertainty of the experiment. Furthermore, changing the point of the wheel that has contact to the cable for every 3 or 4 repetitions is also recommended. Depending on the material being assessed, wearing may easily occur, changing the friction force as the experiments are carried out.

In addition, as highlighted by Boniardi *et al.* (2007), when the failure of aluminium wires in an overhead network of Touggourt Biskra (Algeria) was evaluated, overhead conductors are prone to many degradation phenomena such as repetitive bending and oscillation, corrosion, fatigue and high-frequency vibrations. Those conductors may also have broken or marked strands that may affect the friction coefficient in a specific point of the cable. Therefore, carrying out the measurements for only one region of contact can lead to misunderstanding results. For the results presented in the next section, three different points along the cable were used for the experiments but more contact regions may be assessed. The positions are defined in respect to the higher crossarm. 10 repetitions are made in each position. Besides evaluating friction in distinct regions, measuring in different positions allows to verify the effect of the sag created by the replica's weight in the conductor. The closer to the crossarm, the lesser is the sag.

4. RESULTS AND DISCUSSION

Firstly, the rolling resistance coefficient between the pulley shaft and the bearing was measured, according to the procedure illustrated in Section 3.1 To measure the mass of the containers with water, an electronic digital scale weight SF-400 model is used. This scale has a measuring range from 1 g to 10 kg and a resolution of 1 g. The gravitational acceleration is considered $g = 9.81$ m/s^2. Ten repetitions are performed, resulting in an average friction coefficient of $f_b = 0.1211$, with a standard deviation of 0.0255.

The friction between a wheel's replica and a conductor is studied after estimating the rolling resistance coefficient for the pulley bearing. The proposed procedures were evaluated for a Polyurethane (PU) wheel of 50 Shore A hardness. The same balance used to estimate f_b is used in the experiment. The inclination of the conductor in relation to the ground is measured through the *Pocket Bubble Level* app, an inclinometer app developed by ExaMobile S.A. for smartphones.

Figures 6(a) and (b) illustrate the results obtained by executing the procedure described in Section 3. for three different locations of the aluminium wire. Both static friction and rolling resistance are assessed for the cable in dry and wet conditions. In order to analyse any possible impact of rain into the friction forces, water is poured into the wire until a layer of water is created. The replica is then made wet and positioned in the cable, leaning against the support, exactly as described in the procedure developed.

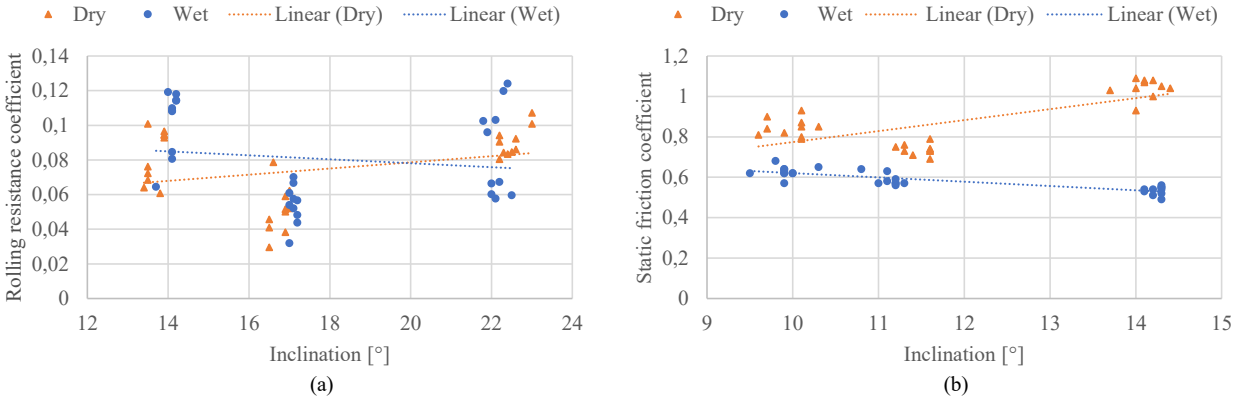

Figure 6. (a) Rolling resistance and (b) static friction coefficients measured in field test.

It can be observed from Fig. 6(a) and (b) that the friction coefficient slightly varies with the increasing of the angle. This variation comes from the dispersion of the data due to observing the wheel motion with an unaided eye. For dry conditions, averages of 0.875 and 0.074 are obtained for the static friction and rolling resistance coefficients, respectively. On the other hand, averages of 0.580 and 0.081 are calculated for the sliding and rolling situations when wet conditions are analysed. As it can be seen in Fig. 6(a), the water almost does not impact the rolling resistance because the wheel expels the water from the region of contact to the wire as it rolls. It is important to highlight, however, that lighter robots or stronger weather conditions may lead to different behaviors. In regard to the sliding of the wheel along the wire, a reduction of 33% in the static friction is observed when raining is simulated, as illustrated by the linear trendlines of Fig. 6(b). The explanation for this situation is that there is a layer of water between the wheel and the wire, acting as lubricant.

5. CONCLUSIONS

This paper presented a method to measure the static friction and rolling resistance coefficients between the surfaces of a wheel and a wire cable. In this work, the method is applied to a replica of the wheel of a robot for inspecting power lines and an aluminum wire cable. Nonetheless, the method can be applied in any environment involving wheels and wire ropes.

The method proved being useful to estimate the coefficients. We could confirm the intuition that water could impact the static friction, aiding to define the robot's operation conditions. Despite the dispersion of the results, their average already helps choosing the motor and evaluating the robot's operation conditions. For applications demanding more precision, some sensors should be used to detect if the wheel starts moving.

Future works include measuring the dynamic friction coefficient, following the standard ABNT NBR 16643; and evaluating rolling resistance through energy conservation and the work done by the rolling resistance force (Minkin and Sikes, 2018).

6. ACKNOWLEDGEMENTS

The R&D project that made this work possible was entitled "Development of a Robotized System for Inspection of Electricity Distribution Lines" (05697-0317 / 2017), regulated by ANEEL ("Agência Nacional de Energia Elétrica") and financed in Florianópolis - Brazil - by Celesc ("Centrais Elétricas de Santa Catarina"). This project is executed by the team of the Laboratory of Applied Robotics (LAR) from the Federal University of Santa Catarina (UFSC) and financially managed by FEESC ("Fundação de Ensino e Engenharia de Santa Catarina"). This study was financed in part by the Coordenação de Aperfeiçoamento de Pessoal de Nível Superior - Brasil (CAPES) - Finance Code 001 and by the Conselho Nacional de Desenvolvimento Científico e Tecnológico (CNPq) [grant number 142193/2018-6]. We are grateful to prof. José Daniel Biasoli de Mello for helping to develop the method.

7. REFERENCES

ABNT NBR 11992, 2017. "Mangueiras de plástico para desobstrução e limpeza de tubulações de pvc rígido por hidrojateamento — determinação do coeficiente de atrito". Standard, Associação Brasileira de Normas Técnicas, Rio de Janeiro, RJ.

ABNT NBR 13989, 1997. "Cabo óptico subterrâneo - determinação do desempenho, quando submetido ao ensaio de coeficiente de atrito estático - método de ensaio". Standard, Associação Brasileira de Normas Técnicas, Rio de Janeiro, RJ.

ABNT NBR 16643, 2017. "Microdutos - coeficiente de atrito - método de ensaio". Standard, Associação Brasileira de Normas Técnicas, Rio de Janeiro, RJ.

ABNT NBR ISO 12957-2, 2013. "Geossintéticos — determinação das características de atrito. parte 2: Ensaio de plano inclinado". Standard, Associação Brasileira de Normas Técnicas, Rio de Janeiro, RJ.

Alhassan, A.B., Zhang, X., Shen, H. and Xu, H., 2020. "Power transmission line inspection robots: A review, trends and challenges for future research". *International Journal of Electrical Power & Energy Systems*, Vol. 118, p. 105862.

Alió-Sanz, J.J., Claros-Stucchi, M., Albaladejo, A., Iglesias-Conde, C. and Alvarado-Lorenzo, A., 2016. "In vitro comparative study on the friction of stainless steel wires with and without orthospeed®(jal 90458) on an inclined plane". *Journal of clinical and experimental dentistry*, Vol. 8, No. 2, p. e141.

ASTM G11510, 2018. "Standard guide for measuring and reporting friction coefficients". Standard, American Society for Testing and Materials, West Conshohocken, PA.

Boje, E., 2014. "Modelling and control of a power supply for a power line inspection robot". In *Proceedings of the 2014 3rd International Conference on Applied Robotics for the Power Industry*. IEEE, pp. 1–6.

Boniardi, M., Cincera, S., D'Errico, F. and Tagliabue, C., 2007. "Fretting fatigue phenomena on an all aluminium alloy conductor". In *Key Engineering Materials*. Trans Tech Publ, Vol. 348, pp. 5–8.

Budinski, K., 2005. "An inclined plane test for the breakaway coefficient of rolling friction of rolling element bearings". *Wear*, Vol. 259, No. 7-12, pp. 1443–1447.

Bühringer, M., Berchtold, J., Büchel, M., Dold, C., Bütikofer, M., Feuerstein, M., Fischer, W., Bermes, C. and Siegwart, R., 2010. "Cable-crawler–robot for the inspection of high-voltage power lines that can passively roll over mast tops". *Industrial Robot: An International Journal*.

Chang, W., Yang, G., Yu, J., Liang, Z., Cheng, L. and Zhou, C., 2017. "Development of a power line inspection robot with hybrid operation modes". In *2017 IEEE/RSJ International Conference on Intelligent Robots and Systems (IROS)*. IEEE, pp. 973–978.

Chang, X.d., Huang, H.b., Peng, Y.x. and Li, S.x., 2020. "Friction, wear and residual strength properties of steel wire rope with different corrosion types". *Wear*, Vol. 458, p. 203425.

Chang, X.d., Peng, Y.x., Zhu, Z.c., Wang, D.g., Gong, X.s., Zou, S.y., Sun, S.s. and Xu, W.x., 2016. "Tribological properties of winding hoisting rope between two layers with different sliding parameters". *Advances in Mechanical Engineering*, Vol. 8, No. 12, p. 1687814016679911.

Debenest, P., Guarnieri, M., Takita, K., Fukushima, E.F., Hirose, S., Tamura, K., Kimura, A., Kubokawa, H., Iwama, N. and Shiga, F., 2008. "Expliner-robot for inspection of transmission lines". In *2008 IEEE International Conference on Robotics and Automation*. IEEE, pp. 3978–3984.

Gao, Y., Song, G., Li, S., Zhen, F., Chen, D. and Song, A., 2020. "Linespyx: A power line inspection robot based on digital radiography". *IEEE Robotics and Automation Letters*, Vol. 5, No. 3, pp. 4759–4765.

Goncalves, R.S. and Carvalho, J.C.M., 2015. "A mobile robot to be applied in high-voltage power lines". *Journal of the Brazilian Society of Mechanical Sciences and Engineering*, Vol. 37, No. 1, pp. 349–359.

Gulzar, M.A., Kumar, K., Javed, M.A. and Sharif, M., 2018. "High-voltage transmission line inspection robot". In *2018 International Conference on Engineering and Emerging Technologies (ICEET)*. IEEE, pp. 1–7.

Li, C., Wu, G. and Cao, H., 2009. "The research on mechanism, kinematics and experiment of 220kv double-circuit transmission line inspection robot". In *International Conference on Intelligent Robotics and Applications*. Springer, pp. 1146–1155.

Minkin, L. and Sikes, D., 2018. "Coefficient of rolling friction-lab experiment". *American Journal of Physics*, Vol. 86, No. 1, pp. 77–78.

Mirallès, F., Hamelin, P., Lambert, G., Lavoie, S., Pouliot, N., Montfrond, M. and Montambault, S., 2018. "Linedrone technology: Landing an unmanned aerial vehicle on a power line". In *2018 IEEE International Conference on Robotics and Automation (ICRA)*. IEEE, pp. 6545–6552.

Montambault, S. and Pouliot, N., 2010. "About the future of power line robotics". In *2010 1st International Conference on Applied Robotics for the Power Industry*. IEEE, pp. 1–6.

Morozovsky, N. and Bewley, T., 2013. "Skysweeper: A low dof, dynamic high wire robot". In *2013 IEEE/RSJ International Conference on Intelligent Robots and Systems*. IEEE, pp. 2339–2344.

Mostashfi, A., Fakhari, A. and Badri, M.A., 2014. "A novel design of inspection robot for high-voltage power lines". *Industrial Robot: An International Journal*.

Nayyerloo, M., Yeganehparast, S.M.M., Barati, A. and Foumani, M.S., 2007. "Mechanical implementation and simulation of mobolab, a mobile robot for inspection of power transmission lines". *International Journal of Advanced Robotic Systems*, Vol. 4, No. 3, p. 41.

Peng, Y.x., Chang, X.d., Sun, S.s., Zhu, Z.c., Gong, X.s., Zou, S.y., Xu, W.x. and Mi, Z.T., 2018. "The friction and wear properties of steel wire rope sliding against itself under impact load". *Wear*, Vol. 400, pp. 194–206.

Pouliot, N. and Montambault, S., 2008. "Geometric design of the linescout, a teleoperated robot for power line inspection and maintenance". In *2008 IEEE International Conference on Robotics and Automation*. IEEE, pp. 3970–3977.

Qing, Z., Xiao-long, Z., Xin-ping, L., Jie, X., Ting, Z. and Cheng-jiang, W., 2016. "Mechanical design and research of a novel power lines inspection robot". In *2016 International Conference on Integrated Circuits and Microsystems (ICICM)*. IEEE, pp. 363–366.

Shakhatreh, H., Sawalmeh, A.H., Al-Fuqaha, A., Dou, Z., Almaita, E., Khalil, I., Othman, N.S., Khreishah, A. and Guizani, M., 2019. "Unmanned aerial vehicles (uavs): A survey on civil applications and key research challenges". *Ieee Access*, Vol. 7, pp. 48572–48634.

Song, Y., Wang, H., Jiang, Y. and Ling, L., 2012. "Aape-d: A novel power transmission line maintenance robot for broken strand repair". In *2012 2nd International Conference on Applied Robotics for the Power Industry (CARPI)*. IEEE, pp. 108–113.

Stawowiak, M. and Żołnierz, M., 2018. "Mobile test stand validation for measuring friction coefficient of carrying rope with friction lining". *Management Systems in Production Engineering*.

Tsujimura, T., Yabuta, T. and Morimitsu, T., 1996. "Design of a wire-suspended mobile robot capable of avoiding path obstacles". *IEE Proceedings-Control Theory and Applications*, Vol. 143, No. 4, pp. 349–357.

Wang, H., Li, E., Yang, G. and Guo, R., 2019. "Design of an inspection robot system with hybrid operation modes for power transmission lines". In *2019 IEEE International Conference on Mechatronics and Automation (ICMA)*. IEEE, pp. 2571–2576.

Xiao, S., Wang, H. and Zhang, J., 2016. "Design and analysis of a novel inspection robot mechanism with assistant arms". In *2016 IEEE International Conference on Cyber Technology in Automation, Control, and Intelligent Systems (CYBER)*. IEEE, pp. 103–108.

Xu, C.m., Peng, Y.x., Zhu, Z.c., Lu, H., Chen, G.a., Wang, D.g., Peng, X. and Wang, S.j., 2019. "Fretting friction and wear of steel wires in tension-torsion and helical contact form". *Wear*, Vol. 432, p. 202946.

Yang, D., Feng, Z. and Zhang, X., 2012. "A novel tribrachiation robot for power line inspection and its inverse kinematics analysis". In *2012 IEEE/ASME International Conference on Advanced Intelligent Mechatronics (AIM)*. IEEE, pp. 502–507.

Yifeng, S., Hongguang, W. and Lie, L., 2011. "Research on the influence of the driving wheel and robot posture on climbing capability of a transmission line inspection robot". In *2011 6th IEEE Conference on Industrial Electronics and Applications*. IEEE, pp. 1632–1639.

Zhang, B., Hou, J., Huang, G., Liu, X., Xue, D. and Wen, X., 2020. "Discussion on a new design of overhead transmission line inspection robot". In *2020 3rd International Conference on Robotics, Control and Automation Engineering (RCAE)*. IEEE, pp. 1–5.

8. RESPONSIBILITY NOTICE

The authors are solely responsible for the printed material included in this paper.